Angela Handlovičová; Karol Mikula

Stability and consistency of the semi-implicit co-volume scheme for regularized mean curvature flow equation in level set formulation

Applications of Mathematics, Vol. 53 (2008), No. 2, 105--129

Persistent URL: `http://dml.cz/dmlcz/134701`

STABILITY AND CONSISTENCY OF THE SEMI-IMPLICIT CO-VOLUME SCHEME FOR REGULARIZED MEAN CURVATURE FLOW EQUATION IN LEVEL SET FORMULATION

Angela Handlovičová, Karol Mikula, Bratislava

(Received June 29, 2006, in revised version July 26, 2007)

Abstract. We show stability and consistency of the linear semi-implicit complementary volume numerical scheme for solving the regularized, in the sense of Evans and Spruck, mean curvature flow equation in the level set formulation. The numerical method is based on the finite volume methodology using the so-called complementary volumes to a finite element triangulation. The scheme gives the solution in an efficient and unconditionally stable way.

Keywords: mean curvature flow, level set equation, numerical solution, semi-implicit scheme, complementary volume method, unconditional stability, consistency

MSC 2000: 35K55, 65M12, 68U10

1. Introduction

The curvature driven level set equation [30]

$$u_t - |\nabla u|\nabla\cdot\Big(\frac{\nabla u}{|\nabla u|}\Big) = 0 \tag{1}$$

as well as its nontrivial generalizations are used in applications as the motion of interfaces (free boundaries) in thermomechanics (solidification, crystal growth) and computational fluid dynamics (free surface flows, multi-phase flows of immiscible fluids, thin films), smoothing and segmentation of images and surface reconstructions in the image processing, computer vision and computer graphics (see e.g. [32], [29], [2], [1], [6], [19], [31], [15], [17]), and in many further situations related to the motion of implicit curves or surfaces. On the other hand, the convergence of numerical schemes to the unique viscosity solution [9], [14], [7] of equation (1) is often an open problem; it is an exception to find an analysis of convergence of the methods used for solving the curvature driven flows in the level set formulation. The level set equation (1) represents the so-called Eulerian approach to curve and surface evolutions. It moves level sets (curves in 2D, surfaces in 3D) of the function u in the normal direction with a velocity proportional to the (mean) curvature. The curves and surfaces are represented implicitly and thus the formulation automatically allows topological changes in the interface which yields robustness of the method.

In [10] Deckelnick and Dziuk prove convergence of their finite element numerical scheme to the solution of the mean curvature flow of graphs which can be further adjusted, using the Evans and Spruck regularization [14], to the situation of motion of level sets by the mean curvature [11]. Convergence of a particular finite difference scheme has been proved by Oberman in [28] using the technique of Barles and Souganidis [3]. More results are available for schemes based on other than level set formulation. The convergent schemes for the so-called direct (parametric, Lagrangean) approach to curvature driven flows were suggested and studied e.g. in [13], [21]; for further Lagrangean methods we refer e.g. to [12], [25], [26]. Other than the level set, but also Eulerian, approach is represented by the phase field method where the convergence of numerical approximation to the solution of the so-called Allen-Cahn equation (modelling diffused interface evolution) is studied, see e.g. [27], [4].

In this paper we prove consistency and stability of the semi-implicit fully discrete complementary volume scheme. Our semi-implicit scheme leads to the solution of linear systems in every discrete time step (for other semi-implicit approaches for solving nonlinear diffusion see e.g. [18], [22], [16], [17]), so it is much more efficient than a fully implicit nonlinear scheme [33], and it is unconditionally stable without any restriction on time step in contrast to many other explicit schemes [30], [32], [29], [31]. Consistency and stability are two properties in the theory of Barles and Souganidis [3] which are used to show convergence of a numerical scheme to solutions of fully nonlinear second order partial differential equations and we discuss them in this paper. Monotonicity is the third question regarding our scheme that still remains open.

The derivation of our numerical method for solving equation (1) is based on the finite volume methodology (see e.g. [20], [22]). We construct the so-called complementary volumes (co-volumes) to a finite element triangulation [33], [16]. Integrating equation (1) in the co-volume gives the weak (integral) formulation of the problem from which the computational scheme naturally follows. One of our main motivations for solving the curvature driven level set equation and its generalizations comes from image processing applications [15], [16], [17], [23], [24], [8]. The co-volume scheme has been applied to smoothing and segmentation of 2D and 3D medical images in [24], [8] and is based on the original semi-implicit method studied in [16]. While in [8] it has been shown experimentally on non-trivial examples of exact solutions that the method converges to the true solution, in this paper we show theoretically its consistency and stability. In the proofs we restrict ourselves to 2D situation and only to the type of grids which we use in image processing applications, cf. the next section, mainly in order to avoid too technical details.

In Section 2 we present in detail our numerical scheme and in Section 3 we prove its properties. For numerical experiments we refer to [16], [24], [23], [8] where co-volume schemes have been applied to problems of interface motion and image smoothing and segmentation.

2. Semi-implicit co-volume scheme

The unknown function $u(t,x)$ in (1) is defined in $Q_T = I \times \Omega$, $\Omega \subset \mathbb{R}^d$ is a bounded Lipschitz domain, $I = [0,T]$ is a time interval, and the equation is usually accompanied with zero Dirichlet (e.g. in image segmentation) or zero Neumann (e.g. in image smoothing) boundary conditions and by an initial condition

$$u(0,x) = u^0(x). \tag{2}$$

To construct the numerical scheme we choose a uniform discrete time step $\tau = T/N$ and replace the time derivative in (1) by the backward difference. The nonlinear terms of the equation are taken from the previous time step while the linear ones are considered on the current time level, which means semi-implicitness of the time discretization.

Semi-implicit in time discretization. Let τ be a given time step and u^0 a given initial level set function. Then, for $n = 1, \dots, N$, we look for a function u^n, a solution of the equation

$$\frac{1}{|\nabla u^{n-1}|} \frac{u^n - u^{n-1}}{\tau} = \nabla \cdot \Big(\frac{\nabla u^n}{|\nabla u^{n-1}|} \Big). \tag{3}$$

Let us introduce now the fully discrete scheme. In the image processing applications, a digital image is given on a structure of pixels with rectangular shape in general (rectangles with solid lines in Fig. 1). Since in every discrete time step of the method (3) we have to evaluate the gradient of the level set function at the previous step $|\nabla u^{n-1}|$, we put a triangulation (dashed lines in Fig. 1) onto the computational domain and then take a piecewise linear approximation of the level set function on

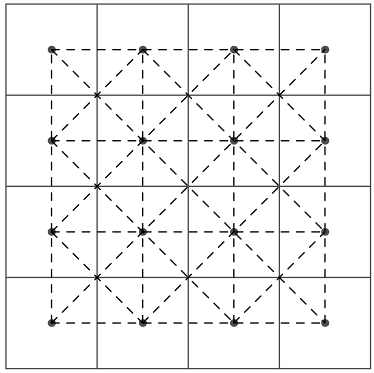

Figure 1. The co-volumes (pixels, solid lines), the triangulation for the co-volume method (dashed lines), and the degree of freedom (DF) nodes (round points).

this triangulation. Such an approach gives a constant value of the gradient per triangle, allowing simple, fast and clear construction of the fully-discrete system of equations.

As can be seen in Fig. 1, in our method the centers of pixels are connected by a new rectangular mesh and every new rectangle is splitted into four triangles. The centers of pixels will be called the degree of freedom (DF) nodes. By this procedure we also get further nodes (at crossings of solid lines in Fig. 1) which, however, will not represent degrees of freedom. We will call them the non-degree of freedom (NDF) nodes. Let a function u be given by discrete values in the DF nodes. Then in the additional NDF nodes we take the average value of the neighboring DF nodal values. By using the so defined values in the NDF nodes, a piecewise linear approximation u_h of u on the triangulation can be built. Let us note that the computational domain Ω is given by the union of all triangles contained in the triangulation $\mathcal{T}_h$ given by the previous construction. It means Ω is equal to the union of all inner pixels and a half-strip of the boundary pixels, cf. Fig. 1. For $\mathcal{T}_h$ we construct a complementary (dual) mesh. We modify the basic approach given in [33], [16] in such a way that our co-volume mesh consists of cells p associated only with the DF nodes p of $\mathcal{T}_h$, say $p = 1, \ldots, M$. Since there will be a one-to-one correspondence between the co-volumes and the DF nodes, without any confusion we can use the same notation for them.

For each DF node p of $\mathcal{T}_h$, let $N(p)$ denote the set of all DF nodes q connected to the node p by an edge. We denote cardinality of this set by N_p. The edge connecting p and q will be denoted by σ_{pq} and its length by h_{pq}. Then every *co-volume* p is bounded by the lines (co-edges) e_{pq} that bisect and are perpendicular to the edges σ_{pq}, $q \in N(p)$. By this construction, the co-volume mesh corresponds exactly to the pixel structure of the image inside the computational domain Ω. We denote by $\mathcal{E}_{pq}$ the set of triangles having σ_{pq} as an edge. In the situation depicted in Fig. 1, every $\mathcal{E}_{pq}$ consists of two triangles. For each $T \in \mathcal{E}_{pq}$ let c_{pq}^T be the length of the portion of e_{pq} that is in T, i.e., $c_{pq}^T = m(e_{pq} \cap T)$, where m is the measure in $\mathbb{R}^{d-1}$. Let $\mathcal{N}_p$ be the set of triangles that have the DF node p as a vertex. Let u_h be a piecewise linear function on the triangulation $\mathcal{T}_h$. We will denote the constant value of $|\nabla u_h|$ on $T \in \mathcal{T}_h$ by $|\nabla u_T|$ and define the regularized gradients by

$$|\nabla u_T|_\varepsilon = \sqrt{\varepsilon^2 + |\nabla u_T|^2}. \tag{4}$$

We will use the notation $u_p = u_h(x_p)$ where x_p is the coordinate of a (DF or NDF) node of the triangulation $\mathcal{T}_h$, and also $u_p^n = u_{h,\tau}(x_p, t_n)$ where $u_{h,\tau}$ is our piecewise linear in space and time approximation of the solution to the regularized level set equation. Let u_h^0 be the piecewise linear interpolation of the initial function u^0 on the triangulation $\mathcal{T}_h$.

With this notation we are ready to derive the co-volume spatial discretization. As is usual in finite volume methods [20], we integrate (3) over every co-volume p, $p = 1, \dots, M$, and then using the divergence theorem we get an integral formulation of (3)

$$\int_p \frac{1}{|\nabla u^{n-1}|} \frac{u^n - u^{n-1}}{\tau} \, \mathrm{d}x = \sum_{q \in N(p)} \int_{e_{pq}} \frac{1}{|\nabla u^{n-1}|} \frac{\partial u^n}{\partial \nu} \, \mathrm{d}s \tag{5}$$

where ν is a unit outer normal to the boundary of p. Now the exact "fluxes" on the right-hand side and the "capacity function" $1/|\nabla u^{n-1}|$ on the left-hand side will be approximated numerically using the piecewise linear reconstruction of u^{n-1} on the triangulation $\mathcal{T}_h$. In such a way, for the approximation of the right-hand side of (5) we get

$$\sum_{q \in N(p)} \left(\sum_{T \in \mathcal{E}_{pq}} c_{pq}^T \frac{1}{|\nabla u_T^{n-1}|} \right) \frac{u_q^n - u_p^n}{h_{pq}}. \tag{6}$$

For the left-hand side of (5) we use

$$m(p) \sum_{T \in \mathcal{N}_p} \frac{m(T \cap p)}{m(p)} \frac{1}{|\nabla u_T^{n-1}|} \frac{u_p^n - u_p^{n-1}}{\tau} \tag{7}$$

where $m(p)$ is the measure in $\mathbb{R}^d$ of the co-volume p. In general, we assume for every pair p, q

$$\underline{h} \leqslant h_{pq} \leqslant \bar{h}, \quad \frac{\bar{h}}{\underline{h}} \leqslant h_0$$

and define

$$d_{pq} := \frac{m(e_{pq})}{h_{pq}} \leqslant d_0. \tag{8}$$

However, we restrict our considerations to uniform rectangular co-volumes with size length h, as plotted in Fig. 1. Then, e.g.,

$$m(p) = h^2, \quad m(e_{pq}) = h_{pq} = h, \quad d_{pq} = 1, \quad c_{pq}^T = \frac{1}{2} m(e_{pq}). \tag{9}$$

We denote four neighbouring DF nodes of x_p by x_{q_1} (east), x_{q_2} (north), x_{q_3} (west), x_{q_4} (south), and the corners of the co-volume p by x_{r_1} (top right), x_{r_2} (top left), x_{r_3} (bottom left), x_{r_4} (bottom right). The middle point of the edge e_{pq_i} is denoted by x_{m_i}, $i = 1, \ldots, 4$.

Taking into account the ε-regularization (4) we can now define coefficients, namely

$$a_{pq}^{n-1} = \frac{1}{|\nabla u_{pq}^{n-1}|_\varepsilon} := \frac{1}{2}\left(\frac{1}{|\nabla u_{T_{pq}^1}^{n-1}|_\varepsilon} + \frac{1}{|\nabla u_{T_{pq}^2}^{n-1}|_\varepsilon}\right), \tag{10}$$

$$b_p^{n-1} := \frac{1}{|\nabla u_p^{n-1}|_\varepsilon} = \frac{1}{N_p} \sum_{q \in N(p)} \frac{1}{|\nabla u_{pq}^{n-1}|_\varepsilon} \tag{11}$$

where $T_{pq}^1, T_{pq}^2 \in \mathcal{E}_{pq}$. For example, for the triangle with vertices x_p, x_{q_1}, x_{r_1} we have

$$|\nabla u_{T_{pq_1}^1}^{n-1}|_\varepsilon = \sqrt{\frac{(u_{q_1} - u_p)^2}{h^2} + \frac{(2(u_{r_1} - u_{m_1}))^2}{h^2} + \varepsilon^2}. \tag{12}$$

Now our computational method can be written as follows.

Fully-discrete semi-implicit co-volume scheme. Let u_p^0, $p = 1, \ldots, M$ be given discrete initial values of the segmentation function. Then for $n = 1, \ldots, N$ we look for u_p^n, $p = 1, \ldots, M$ satisfying

$$b_p^{n-1} m(p) u_p^n + \tau \sum_{q \in N(p)} a_{pq}^{n-1} d_{pq} (u_p^n - u_q^n) = b_p^{n-1} m(p) u_p^{n-1}. \tag{13}$$

Remark 2.1. The co-volume algorithms [33], [16] studied previously for the level-set-like problems have used either "left oriented" or "right oriented" triangulations and no NDF nodes (see Fig. 2). However, then the level set curve or surface evolution is influenced by the grid effect. Of course this effect is satisfactory weakened by refining the grid (e.g. in interface motion computations, cf. [16]). In image processing we work with fixed given pixel/voxel structure, and we do not refine this structure, so we want to remove such "non-symmetry" of the method. This can be done by averaging the two, "left" and "right" solutions, or implicitly by taking the combination of triangulations as plotted in Fig. 1. Of course, usage of such a "symmetric" triangulation can be accompanied also by the linear finite element method of Deckelnick and Dziuk [10], [11], considering also the NDF nodes as degrees of freedom. But this would increase the number of unknowns in systems to be solved by factor two, which can be critical in case of image processing applications, usually with a huge number of pixels/voxels given. Without any construction of a triangulation, we could also use a bi-linear representation of the level set function on finite elements corresponding to the rectangular grid formed by the centers of pixels and build a tensor-product finite element method. But then we would face a problem of non-constant gradients in the evaluation of nonlinearities. The same problem would arise when considering the complementary volume method given by the dual grid corresponding to pixels and by a bi-linear representation of the function on the rectangular grid formed by centers of pixels. Again, such technique would require the evaluation and integration of the absolute value of the gradient of bi-linear functions on the co-volume sides. From the above points of view, our method gives the smallest possible number of unknowns and the simplest (piecewise constant) nonlinear coefficients evaluation.

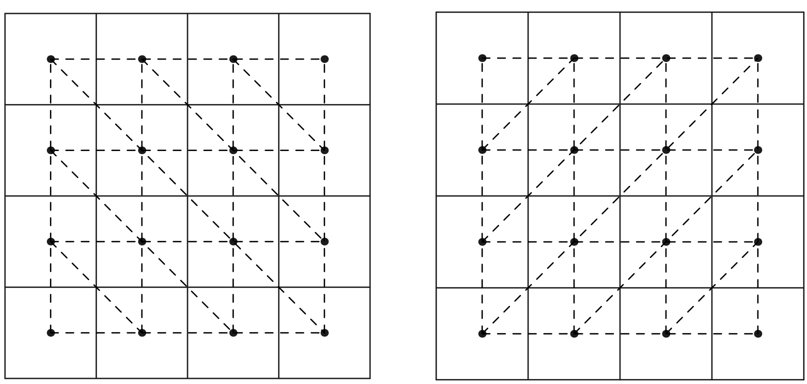

Figure 2. By dashed lines we plot the "left oriented" triangulation (left) and the "right oriented" triangulation (right). The "symmetric" triangulation corresponding to our method is plotted in Fig. 1.

Such a "symmetric" primal-dual grid can be built also in three dimensions. The construction of a co-volume mesh in 3D has to use the 3D tetrahedral finite element grid to which it is complementary. For this goal we use the following approach similar to the so called centered-cubic-lattice method known from computer graphics [5].

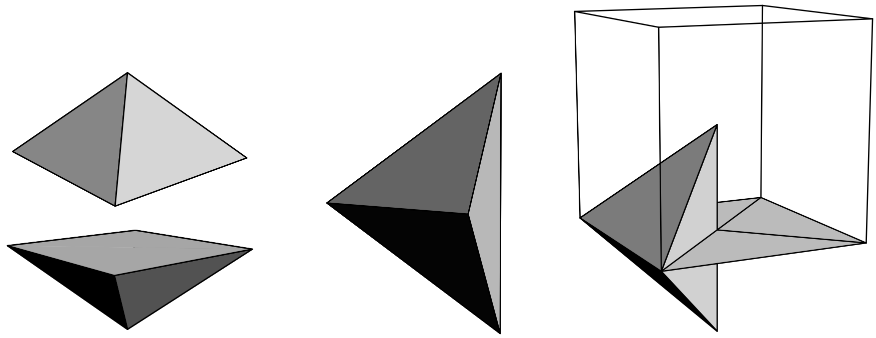

Figure 3. Neighbouring pyramids which are joined together (left); joining these pyramids and then splitting them into four parts give a tetrahedron of the 3D grid (middle); the intersection of the tetrahedron with the bottom face of the co-volume (right).

First, every cubic voxel is splitted into 6 pyramids with their vertex given by the voxel center and their base surfaces given by the voxel boundary faces. The neighbouring pyramids of neighbouring voxels are joined together to form an octahedron which is then splitted into 4 tetrahedrons using diagonals of the voxel boundary face—see Fig. 3. In this way we get a 3D tetrahedral grid. Two nodes of every tetrahedron correspond to the centers of the neighbouring voxels and the other two nodes correspond to the voxel boundary vertices; every tetrahedron intersects the common face of neighbouring voxels. Now again only the centers of voxels represent DF nodes, the additional nodes of tetrahedrons are NDF nodes which are used only in piecewise linear representation of the level set function. Using such co-volumes one obtains a computational scheme with the same structure as (13) but the averages in definitions (10), (11) are taken over all tetrahedrons crossing the faces and the entire co-volume, respectively.

3. Consistency and stability of the numerical scheme

We first give the necessary notation and definitions. Let us assume that $\varepsilon > 0$ is fixed. The Evans and Spruck regularization of the curvature driven level set equation (1) can be written in the form

$$u_t - \operatorname{trace}\Big(\Big(\mathbf{I} - \frac{\nabla u \otimes \nabla u}{|\nabla u|_\varepsilon^2}\Big)\overline{D}^2 u\Big) = 0 \quad \text{in } I \times \Omega \tag{14}$$

where $\overline{D}^2 u$ denotes the symmetric matrix of the second order spatial derivatives of u. If we denote

$$G(\mathbf{X}, p) = \operatorname{trace}\Big(\Big(\mathbf{I} - \frac{p \otimes p}{|p|_\varepsilon^2}\Big) \cdot \mathbf{X}\Big),$$

where $(\mathbf{X}, p) \in \mathbf{S}^d \times \mathbb{R}^d$ and $\mathbf{S}^d$ is the space of $d \times d$ symmetric matrices, then G is an elliptic operator [9]. We denote by $B(Q)$, $Q = I \times \bar{\Omega}$, the set of all uniformly bounded functions in a domain Q. In [14], existence of the unique smooth solution is proved.

Let us consider the equation

$$F(D^2u, Du, u) = 0 \quad \text{in } Q \tag{15}$$

where in the spatially two dimensional case we define

$$Du = \begin{pmatrix} u_t \\ u_x \\ u_y \end{pmatrix}, \quad D^2u = \begin{pmatrix} u_{tt} & u_{tx} & u_{ty} \\ u_{tx} & u_{xx} & u_{xy} \\ u_{ty} & u_{xy} & u_{yy} \end{pmatrix}, \quad \bar{\mathcal{I}} = \begin{pmatrix} 0 & 0 & 0 \\ 0 & 1 & 0 \\ 0 & 0 & 1 \end{pmatrix}, \quad \bar{I} = \begin{pmatrix} 1 \\ 0 \\ 0 \end{pmatrix}$$

and $F\colon \mathbf{S}^d \times \mathbb{R}^d \times \mathbb{R} \to \mathbb{R}$ is given by

$$F(D^2u, Du, u) = \begin{cases} \bar{I} \cdot Du - \operatorname{trace}\Bigl(\Bigl(\bar{\mathcal{I}} - \dfrac{(\bar{\mathcal{I}} \cdot Du) \otimes (\bar{\mathcal{I}} \cdot Du)}{|\bar{\mathcal{I}} \cdot Du|_\varepsilon^2}\Bigr) D^2u\Bigr) & \text{in } Q, \\ u(0,x) - u^0(x) \quad \text{in } \Omega, \\ \dfrac{\partial u}{\partial \nu} \quad \text{or } u \quad \text{on } I \times \partial\Omega \end{cases}$$

where ν is an outer unit normal to $\partial\Omega$. It is now clear from the properties of G above that F possesses the elliptic property, that means, for all $(p, u) \in \mathbb{R}^d \times \mathbb{R}$ and for all $\mathbf{M}, \mathbf{N} \in \mathbf{S}^d$ we have

$$F(\mathbf{M}, p, u) \leqslant F(\mathbf{N}, p, u) \quad \text{provided } \mathbf{M} \geqslant \mathbf{N}.$$

Let us have an approximation scheme of the form

$$S(\varrho, Y, u^\varrho(Y), u^\varrho) = 0 \quad \text{in } Q \tag{16}$$

where $S\colon \mathbb{R}^+ \times Q \times \mathbb{R} \times B(Q) \to \mathbb{R}$ is locally uniformly bounded.

Definition 3.1. The approximation scheme S given by (16) has the *monotonicity* property if for all $\varrho \geqslant 0$, $Y \in Q$, $\zeta \in \mathbb{R}$ and $u, v \in B(Q)$ the inequality $u \geqslant v$ implies

$$S(\varrho, Y, \zeta, u) \leqslant S(\varrho, Y, \zeta, v). \tag{17}$$

Definition 3.2. The approximation scheme S given by (16) has the *stability* property if for all $\varrho > 0$ there exists a solution

$$u^\varrho \in B(Q) \tag{18}$$

of (16) with a bound independent of ϱ.

Definition 3.3. The approximation scheme S given by (16) has the *consistency* property if for all $\Phi \in C^\infty(Q)$ and for all $X \in Q$ we have

$$\lim_{\varrho\to 0,\, Y\to X,\, \xi\to 0} \frac{S(\varrho, Y, \Phi(Y)+\xi, \Phi+\xi)}{\varrho} = F(D^2\Phi(X), D\Phi(X), \Phi(X)). \tag{19}$$

We recall the following important statement:

Theorem 3.1 ([3]). *Let the approximation scheme S given by* (16) *have the stability, monotonicity and consistency properties. Then, as $\varrho \to 0$, the solution of the scheme converges locally uniformly to the unique continuous solution of* (15).

Our aim is to transform the numerical scheme (13) to the form (16) and then prove the stability and consistency properties. The numerical scheme (13) can be written in the form (16) provided $\varrho = \tau$, $Y = (t_n, x_p)$, $u^\varrho(Y) = u_p^n$, $u^\varrho = u_{h,\tau}$ where $u_{h,\tau}(x, y)$ is a piecewise linear in space and time (i.e. on the triangulation $\mathcal{T}_h$ and among discrete time steps) approximation of solution, and

$$S(\varrho, (t_n, x_p), u_p^n, u_{h,\tau}) = u_p^n - u_p^{n-1} + \frac{\tau}{b_p^{n-1} m(p)} \sum_{q\in N(p)} a_{pq}^{n-1}(u_p^n - u_q^n) d_{pq} = 0 \tag{20}$$

where $u_p^0 = u_0(x_p)$ for all $p = 1, \ldots, M$. Let us note that the time step τ is usually coupled with the spatial step h, e.g., by the relation $\tau \approx h^2$ which is natural in solving parabolic PDEs.

The zero Neumann boundary conditions are realized using the mirror image extension of the solution values outside the image domain, i.e., adding one outer strip of pixels (co-volumes) q along the boundary pixels p, cf. Fig. 1, and prescribing $u_q^n = u_p^n$ for these additional pixel values. The result is that the boundary terms $a_{pq}^{n-1}(u_p^n - u_q^n)d_{pq}$ are simply not present in the summation term of the scheme (13) or in its equivalent form (20), which is also equivalent to prescribing $a_{pq}^{n-1} = 0$ if p is a boundary co-volume and q is an additional one.

Since we assume that the computational domain Ω is given by the union of all triangles in $\mathcal{T}_h$, cf. Fig. 1, the DF nodes of boundary pixels lie on $\partial\Omega$ and we prescribe zero values to them in case of the Dirichlet boundary condition. The only change in the scheme is that the system contains less number of unknowns (only DF nodes of inner pixels) and that $a_{pq}^{n-1}(u_p^n - u_q^n)d_{pq}$ in the summation term contain the known value $u_q^n = 0$ if q is a boundary pixel.

Theorem 3.2. *There exists a unique solution* $u_h^n = (u_1^n, \ldots, u_M^n)$ *of the scheme* (13) *for any value of the regularization parameter* $\varepsilon > 0$ *and for any time step* $n = 1, \ldots, N$. *Moreover, for the fully discrete numerical solution* $u_{h,\tau}$ *the estimate*

$$\|u_{h,\tau}\|_{L_\infty(Q)} \leqslant \|u_h^0\|_{L_\infty(\bar{\Omega})} \tag{21}$$

holds, which gives the stability property of the scheme.

Proof. It follows from definition (10) that the off-diagonal elements $-\tau a_{pq}^{n-1}$, $q \in N(p)$, of the system (13) are symmetric and nonpositive. The positive term b_p^{n-1} given by (11) affects only the diagonal which is equal to $b_p^{n-1} m(p) + \tau \sum\limits_{q \in N(p)} a_{pq}^{n-1} d_{pq}$. Thus, the matrix of the system (13) is a symmetric and diagonally dominant M-matrix which implies that it always has a unique solution. Let us write (13) in the form (20)

$$u_p^n + \frac{\tau}{b_p^{n-1} m(p)} \sum_{q \in N(p)} a_{pq}^{n-1} (u_p^n - u_q^n) d_{pq} = u_p^{n-1} \tag{22}$$

and let $\max u_h^n = \max(u_1^n, \ldots, u_M^n)$ be achieved at the point p.

In the case of the zero Neumann boundary condition, no matter whether p is an inner or a boundary point, the whole second term on the left-hand side of (22) is nonnegative and thus $u_p^n \leqslant u_p^{n-1} \leqslant \max(u_1^{n-1}, \ldots, u_M^{n-1})$. In the same way we can prove a similar relation for the minima and together we have

$$\min u_p^0 \leqslant \min u_p^n \leqslant \max u_p^n \leqslant \max u_p^0, \quad n \leqslant N, \tag{23}$$

which implies the estimate (21).

In the case of the zero Dirichlet boundary condition, first let p be a boundary DF node in which the maximum of the discrete solution is attained at the nth time step (this maximum is of course equal to 0). It is clear that it is less than or equal to the maximum at the previous time step $n-1$, which can be either positive (if realized in an inner node) or zero (if realized in a boundary node). Secondly, if p is an inner node, similarly to the considerations for the Neumann boundary condition above, we have that the whole second term on the left-hand side of (22) is nonnegative and thus $u_p^n \leqslant u_p^{n-1}$ which is less or equal to the maximum at the time step $n-1$. Then we get recursively the estimate (21) again. □

Theorem 3.3. *For any fixed $\varepsilon > 0$ our numerical scheme possesses the consistency property.*

Proof. Let $X = (t, x)$ and $\Phi \in C^\infty(Q)$. There exists a time step $n \in \{0, 1, \dots N\}$ such that $t \in \langle t_{n-1}, t_n\rangle$ and a co-volume $p \in \{1, \dots M\}$ such that $x \in p$. We denote $Y = (t_n, x_p)$, and $\Phi_p^n := \Phi(t_n, x_p)$. In order to get consistency, in our case it is sufficient to prove the existence of positive integers k_1, k_2 such that

$$\left|\frac{S(\varrho, Y, \Phi(Y), \Phi)}{\varrho} - F(D^2\Phi(X), D\Phi(X), \Phi(X))\right| \leqslant C(\|\Phi\|_3)(\tau^{k_1} + h^{k_2})$$

where by $\|\Phi\|_k$ we denote the norm of the functional space $C^k(Q)$ and $C(\|\Phi\|_3)$ is a constant which can depend on a $C^3(Q)$ norm of the smooth function Φ. For our scheme it can be written in the form

$$\begin{aligned}\left|\frac{\Phi_p^n - \Phi_p^{n-1}}{\tau} - \frac{1}{b_p^{n-1} m(p)} \sum_{q\in N(p)} a_{pq}^{n-1}(\Phi_q^n - \Phi_p^n) - \Phi_t(X)\right.&\\ \left. + |\nabla\Phi(X)|_\varepsilon \nabla\cdot \frac{\nabla\Phi(X)}{|\nabla\Phi(X)|_\varepsilon}\right|&\\ \leqslant C(\|\Phi\|_3)(\tau^{k_1} + h^{k_2}).&\end{aligned} \tag{24}$$

We will prove inequality (24) by subsequently estimating the differences of particular terms on the left-hand side. Since $\Phi \in C^\infty(Q)$ it is clear that

$$\frac{\Phi_p^n - \Phi_p^{n-1}}{\tau} = \Phi_t(\xi, x_p)$$

where $\xi \in \langle t_{n-1}, t_n\rangle$. Because $|\xi - t| \leqslant \tau$ and $|x - x_p| \leqslant \sqrt{2}h$ we have

$$\left|\frac{\Phi_p^n - \Phi_p^{n-1}}{\tau} - \Phi_t(X)\right| \leqslant |\Phi_t(\xi, x_p) - \Phi_t(t, x)| \leqslant C(\|\Phi\|_2)(\tau + h).$$

The second term in (24) can be rewritten in the form

$$II = -\frac{1}{b_p^{n-1} m(p)} \sum_{q\in N(p)} \int_{e_{pq}} a_{pq}^{n-1} \frac{\Phi_q^n - \Phi_p^n}{h}\, \mathrm{d}s.$$

Let us omit, for a moment, the upper time index for Φ, and let us use on each edge e_{pq} for the difference term $(\Phi_q - \Phi_p)/h$ the Taylor expansion in a way similar to that used to derive the usual central difference approximation. Let $x_p = (x_{1p}, x_{2p})$

and $x_{q_i} = (x_{1q_i}, x_{2q_i})$ for $i = 1, \dots, 4$. Let $s = (s_1, s_2)$ be a point on the boundary of the co-volume p. Then

$$\text{for a point } s \in e_{pq_1} \text{ we have } s = \Big(x_{1p} + \frac{h}{2}, x_{2p} + t\frac{h}{2}\Big), \quad t \in \langle -1, 1\rangle\,, \tag{25}$$

$$\text{for a point } s \in e_{pq_2} \text{ we have } s = \Big(x_{1p} + t\frac{h}{2}, x_{2p} + \frac{h}{2}\Big), \quad t \in \langle -1, 1\rangle\,, \tag{26}$$

$$\text{for a point } s \in e_{pq_3} \text{ we have } s = \Big(x_{1p} - \frac{h}{2}, x_{2p} + t\frac{h}{2}\Big), \quad t \in \langle -1, 1\rangle\,, \tag{27}$$

$$\text{for a point } s \in e_{pq_4} \text{ we have } s = \Big(x_{1p} + t\frac{h}{2}, x_{2p} - \frac{h}{2}\Big), \quad t \in \langle -1, 1\rangle\,. \tag{28}$$

Then for e_{pq_1} and e_{pq_3} we have

$$\frac{\Phi_q - \Phi_p}{h} = \frac{\partial \Phi(s)}{\partial \nu} + 2\Phi_{xy}(s) \cdot \operatorname{sgn}(x_{1q} - x_{1p})(x_{2q} - s_2) + O(h^2) \tag{29}$$

and for e_{pq_2} and e_{pq_4} similarly

$$\frac{\Phi_q - \Phi_p}{h} = \frac{\partial \Phi(s)}{\partial \nu} + 2\Phi_{xy}(s) \cdot \operatorname{sgn}(x_{2q} - x_{2p})(x_{1q} - s_1) + O(h^2). \tag{30}$$

Involving these relations in term II and using

$$\frac{\sum\limits_{q \in N(p)} a_{pq}^{n-1}(w)}{b_p^{n-1}(w)} = 4 \tag{31}$$

which holds for any function $w \in B(Q)$ on a uniform rectangular grid due to (10)–(11), we obtain

$$\begin{aligned}
II = &- \frac{1}{b_p^{n-1} m(p)} \sum_{q=1,3} \int_{e_{pq}} a_{pq}^{n-1} \Big(\frac{\partial \Phi(s)}{\partial \nu} + 2\Phi_{xy}(s) \cdot \operatorname{sgn}(x_{1q} - x_{1p}) \\
&\qquad\qquad\qquad\qquad\qquad\qquad \times (x_{2q} - s_2)\Big)\, \mathrm{d}s \\
&- \frac{1}{b_p^{n-1} m(p)} \sum_{q=2,4} \int_{e_{pq}} a_{pq}^{n-1} \Big(\frac{\partial \Phi(s)}{\partial \nu} + 2\Phi_{xy}(s) \cdot \operatorname{sgn}(x_{2q} - x_{2p})(x_{1q} - s_1)\Big)\, \mathrm{d}s \\
&\qquad\qquad\qquad\qquad\qquad\qquad + C(\|\Phi\|_3)h \\
= &- \frac{1}{b_p^{n-1} m(p)} \sum_{q \in N(p)} \int_{e_{pq}} a_{pq}^{n-1} \frac{\partial \Phi(s)}{\partial \nu}\, \mathrm{d}s \\
&- \frac{1}{b_p^{n-1} m(p)} \sum_{q=1,3} \int_{e_{pq}} a_{pq}^{n-1} 2\Phi_{xy}(s) \cdot \operatorname{sgn}(x_{1q} - x_{1p})(x_{2q} - s_2)\, \mathrm{d}s \\
&- \frac{1}{b_p^{n-1} m(p)} \sum_{q=2,4} \int_{e_{pq}} a_{pq}^{n-1} 2\Phi_{xy}(s) \cdot \operatorname{sgn}(x_{1q} - x_{1p})(x_{2q} - s_2)\, \mathrm{d}s + C(\|\Phi\|_3)h \\
= &\, II_1 + II_2 + II_3 + C(\|\Phi\|_3)h.
\end{aligned}$$

Using parametrizations (25)–(28) we can rearrange term II_2 (term II_3 can be estimated analogously) on the edge e_{pq_1} into the form

$$-\frac{2h}{2b_p^{n-1}m(p)}\int_{-1}^{1} a_{pq_1}^{n-1}\Phi_{xy}\Big(x_{1p}+\frac{h}{2}, x_{2p}+t\frac{h}{2}\Big)\Big(-t\frac{h}{2}\Big)\,\mathrm{d}t$$

and on the edge e_{pq_3} similarly

$$-\frac{2h}{2b_p^{n-1}m(p)}\int_{-1}^{1} a_{pq_3}^{n-1}\Phi_{xy}\Big(x_{1p}-\frac{h}{2}, x_{2p}+t\frac{h}{2}\Big)\Big(t\frac{h}{2}\Big)\,\mathrm{d}t.$$

We can collect these two terms together, and using the fact that $\Phi \in C^\infty(Q)$ we have

$$\begin{aligned}|II_2| &\leqslant \Big|\frac{h^2}{2b_p^{n-1}m(p)}\int_{-1}^{1} t(a_{pq_1}^{n-1}-a_{pq_3}^{n-1})\Phi_{xy}\Big(x_{1p}+\frac{h}{2}, x_{2p}+t\frac{h}{2}\Big)\,\mathrm{d}t \\ &\quad + \frac{h^2}{2b_p^{n-1}m(p)}\int_{-1}^{1} t a_{pq_3}^{n-1}\Big(\Phi_{xy}\Big(x_{1p}+\frac{h}{2}, x_{2p}+t\frac{h}{2}\Big) \\ &\qquad\qquad - \Phi_{xy}\Big(x_{1p}-\frac{h}{2}, x_{2p}+t\frac{h}{2}\Big)\Big)\,\mathrm{d}t\Big| \\ &\leqslant \|\Phi\|_2\frac{|a_{pq_1}^{n-1}-a_{pq_3}^{n-1}|}{2b_p^{n-1}} + C(\|\Phi\|_3)\frac{a_{pq_3}^{n-1}}{2b_p^{n-1}}h.\end{aligned}$$

Putting all together we obtain

$$\begin{aligned}|II_2|+|II_3| &\leqslant C(\|\Phi\|_2)h\frac{a_{pq_3}^{n-1}+a_{pq_4}^{n-1}}{b_p^{n-1}} \\ &\quad + C(\|\Phi\|_3)\frac{|a_{pq_1}^{n-1}-a_{pq_3}^{n-1}|+|a_{pq_2}^{n-1}-a_{pq_4}^{n-1}|}{b_p^{n-1}}.\end{aligned} \tag{32}$$

The first term on the right-hand side can be estimated using (31) and we obtain an $O(h)$ term. In the second term we estimate the difference $a_{pq_1}^{n-1}-a_{pq_3}^{n-1}$ (further part can be treated analogously). We have

$$|a_{pq_1}^{n-1}-a_{pq_3}^{n-1}| = \frac{1}{2}\Big|\frac{1}{|\nabla\Phi_{T_{11}}|_\varepsilon}+\frac{1}{|\nabla\Phi_{T_{12}}|_\varepsilon}-\frac{1}{|\nabla\Phi_{T_{31}}|_\varepsilon}-\frac{1}{|\nabla\Phi_{T_{32}}|_\varepsilon}\Big| \tag{33}$$

where $T_{11}=T_{pq_1}^1$, $T_{12}=T_{pq_1}^2$ are two triangles corresponding to the points x_p, x_{q_1} and $T_{31}=T_{pq_3}^1$, $T_{32}=T_{pq_3}^2$ are two triangles corresponding to the points x_p, x_{q_3}. We can put together terms with T_{11} and T_{31} (analogously it can be done for terms with T_{12} and T_{32}) and then use our approximation of the gradient, cf. (12), to get

$$\begin{aligned}\frac{1}{|\nabla\Phi_{T_{11}}|_\varepsilon}-\frac{1}{|\nabla\Phi_{T_{31}}|_\varepsilon} &= \frac{|\nabla\Phi_{T_{11}}|^2-|\nabla\Phi_{T_{31}}|^2}{|\nabla\Phi_{T_{11}}|_\varepsilon|\nabla\Phi_{T_{31}}|_\varepsilon(|\nabla\Phi_{T_{11}}|_\varepsilon+|\nabla\Phi_{T_{31}}|_\varepsilon)}\\ &= \frac{(\Phi(x_{q_1})-\Phi(x_p))^2-(\Phi(x_{q_3})-\Phi(x_p))^2}{h^2|\nabla\Phi_{T_{11}}|_\varepsilon|\nabla\Phi_{T_{31}}|_\varepsilon(|\nabla\Phi_{T_{11}}|_\varepsilon+|\nabla\Phi_{T_{31}}|_\varepsilon)}\\ &\quad+\frac{(2(\Phi(x_{r_1})-\Phi(x_{m_1})))^2-(2(\Phi(x_{r_2})-\Phi(x_{m_3})))^2}{h^2|\nabla\Phi_{T_{11}}|_\varepsilon|\nabla\Phi_{T_{31}}|_\varepsilon(|\nabla\Phi_{T_{11}}|_\varepsilon+|\nabla\Phi_{T_{31}}|_\varepsilon)}.\end{aligned}$$

Because of the properties of Φ we have

$$\begin{aligned}&\frac{\Phi(x_{q_1})-\Phi(x_p)}{h}=\Phi_x(\xi),\quad \frac{\Phi(x_{q_3})-\Phi(x_p)}{h}=\Phi_x(\eta),\\ &\frac{2(\Phi(x_{r_1})-\Phi(x_{m_1}))}{h}=\Phi_y(\zeta),\quad \frac{2(\Phi(x_{r_2})-\Phi(x_{m_3}))}{h}=\Phi_y(\theta)\end{aligned}\tag{34}$$

where ξ lies on the abscissa with end points x_p, x_{q_1}, η lies on the abscissa with end points x_p, x_{q_3}, ζ lies on the abscissa with end points x_{m_1}, x_{r_1} and θ lies on the abscissa with end points x_{m_3}, x_{r_2}. Employing these facts and again the smoothness properties of Φ we obtain

$$\begin{aligned}&\left|\frac{1}{|\nabla\Phi_{T_{11}}|_\varepsilon}-\frac{1}{|\nabla\Phi_{T_{31}}|_\varepsilon}\right|\\ &\qquad\leqslant\frac{|(\Phi_x(\xi)-\Phi_x(\eta))(\Phi_x(\xi)+\Phi_x(\eta))|+|(\Phi_y(\zeta)-\Phi_y(\theta))(\Phi_y(\zeta)+\Phi_y(\theta))|}{|\nabla\Phi_{T_{11}}|_\varepsilon|\nabla\Phi_{T_{31}}|_\varepsilon(|\nabla\Phi_{T_{11}}|_\varepsilon+|\nabla\Phi_{T_{31}}|_\varepsilon)}\\ &\qquad\leqslant\frac{\sqrt{2}\|\Phi\|_2h(|\nabla\Phi_{T_{11}}|+|\nabla\Phi_{T_{31}}|)}{|\nabla\Phi_{T_{11}}|_\varepsilon|\nabla\Phi_{T_{31}}|_\varepsilon(|\nabla\Phi_{T_{11}}|_\varepsilon+|\nabla\Phi_{T_{31}}|_\varepsilon)}\\ &\qquad\leqslant\frac{C(\|\Phi\|_3)h}{|\nabla\Phi_{T_{11}}|_\varepsilon|\nabla\Phi_{T_{31}}|_\varepsilon}.\end{aligned}$$

If we estimate also the difference for terms with T_{12} and T_{32} in (33) and similarly the term $\left|a^{n-1}_{pq_2}-a^{n-1}_{pq_4}\right|$ in (32) we finally arrive at

$$\begin{aligned}|II_2|+|II_3|&\leqslant C(\|\Phi\|_3)h+\frac{C(\|\Phi\|_3)h}{b_p^{n-1}}\Big(\frac{1}{|\nabla\Phi_{T_{11}}|_\varepsilon|\nabla\Phi_{T_{31}}|_\varepsilon}+\frac{1}{|\nabla\Phi_{T_{12}}|_\varepsilon|\nabla\Phi_{T_{32}}|_\varepsilon}\\ &\qquad+\frac{1}{|\nabla\Phi_{T_{21}}|_\varepsilon|\nabla\Phi_{T_{41}}|_\varepsilon}+\frac{1}{|\nabla\Phi_{T_{22}}|_\varepsilon|\nabla\Phi_{T_{42}}|_\varepsilon}\Big)\\ &\leqslant C(\|\Phi\|_3)h+\frac{C(\|\Phi\|_3)h}{\varepsilon}.\end{aligned}$$

Now, term II_1 can be written as

$$
\begin{aligned}
II_1 = & -\frac{1}{b_p^{n-1}m(p)} \sum_{q\in N(p)} \int_{e_{pq}} a_{pq}^{n-1} \frac{\partial \Phi(t_n,s)}{\partial \nu}\,\mathrm{d}s \\
= & -\frac{1}{b_p^{n-1}m(p)} \sum_{q\in N(p)} \int_{e_{pq}} \frac{1}{|\nabla\Phi(t_{n-1},s)|_\varepsilon} \frac{\partial \Phi(t_n,s)}{\partial \nu}\,\mathrm{d}s \\
& -\frac{1}{b_p^{n-1}m(p)} \sum_{q\in N(p)} \int_{e_{pq}} \Big(a_{pq}^{n-1} - \frac{1}{|\nabla\Phi(t_{n-1},s)|_\varepsilon}\Big) \frac{\partial \Phi(t_n,s)}{\partial \nu}\,\mathrm{d}s = III_1 + III_2.
\end{aligned}
$$

An approach similar to the above can also be used to estimate term III_2. We again for a moment omit the time variable in the function Φ and estimate the terms along the opposite sides of the co-volume p boundary. Then for the edge e_{pq_1} we have

$$
a_{pq_1}^{n-1} - \frac{1}{|\nabla\Phi(s)|_\varepsilon} = \frac{1}{2}\Big(\frac{1}{|\nabla\Phi_{T_{11}}|_\varepsilon} - \frac{1}{|\nabla\Phi(s)|_\varepsilon}\Big) + \frac{1}{2}\Big(\frac{1}{|\nabla\Phi_{T_{12}}|_\varepsilon} - \frac{1}{|\nabla\Phi(s)|_\varepsilon}\Big),
$$

and now we rearrange the first term containing T_{11} as follows:

$$
\begin{aligned}
\frac{1}{|\nabla\Phi(s)|_\varepsilon} - \frac{1}{|\nabla\Phi_{T_{11}}|_\varepsilon} &= \frac{|\nabla\Phi_{T_{11}}|^2 - |\nabla\Phi(s)|^2}{|\nabla\Phi_{T_{11}}|_\varepsilon |\nabla\Phi(s)|_\varepsilon (|\nabla\Phi_{T_{11}}|_\varepsilon + |\nabla\Phi(s)|_\varepsilon)} \\
&= \frac{((\Phi_{q_1} - \Phi_p)/h)^2 - (\Phi_x(s))^2 + (2(\Phi_{r_1} - \Phi_{m_1})/h)^2 - (\Phi_y(s))^2}{|\nabla\Phi_{T_{11}}|_\varepsilon |\nabla\Phi(s)|_\varepsilon (|\nabla\Phi_{T_{11}}|_\varepsilon + |\nabla\Phi(s)|_\varepsilon)} \\
&= \frac{((\Phi_{q_1} - \Phi_p/)h - \Phi_x(s))((\Phi_{q_1} - \Phi_p/)h + \Phi_x(s))}{|\nabla\Phi_{T_{11}}|_\varepsilon |\nabla\Phi(s)|_\varepsilon (|\nabla\Phi_{T_{11}}|_\varepsilon + |\nabla\Phi(s)|_\varepsilon)} \\
&\quad + \frac{(2(\Phi_{r_1} - \Phi_{m_1})/h - \Phi_y(s))(2(\Phi_{r_1} - \Phi_{m_1})/h + \Phi_y(s))}{|\nabla\Phi_{T_{11}}|_\varepsilon |\nabla\Phi(s)|_\varepsilon (|\nabla\Phi_{T_{11}}|_\varepsilon + |\nabla\Phi(s)|_\varepsilon)}.
\end{aligned}
$$

We apply again the Taylor expansion using the parametrization (25) and get

$$
\begin{aligned}
\frac{\Phi_{q_1} - \Phi_p}{h} - \Phi_x(s) &= 2\Phi_{xy}(s)t\frac{h}{2} + O(h^2), \\
\frac{2(\Phi_{r_1} - \Phi_{m_1})}{h} - \Phi_y(s) &= \Phi_{yy}(s)\frac{h}{2}(1-2t) + O(h^2),
\end{aligned}
$$

and the same can be done also for the second term containing T_{12}. Now we introduce some notation to simplify integrals in term III_2. For both triangles T_{1i}, $i = 1, 2$ we define

$$
\begin{aligned}
n_{1i}(s) &= \Big(2\Phi_{xy}(s)t\frac{h}{2} + O(h^2)\Big)\Big(\frac{\Phi_{q_1} - \Phi_p}{h} + \Phi_x(s)\Big), \\
m_{1i}(s) &= \Big(\Phi_{yy}(s)\frac{h}{2}(1-2t) + O(h^2)\Big)\Big(\frac{2(\Phi_{r_1} - \Phi_{m_1})}{h} + \Phi_y(s)\Big), \\
p_{1i}(s) &= |\nabla\Phi_{T_{1i}}|_\varepsilon |\nabla\Phi(s)|_\varepsilon (|\nabla\Phi_{T_{1i}}|_\varepsilon + |\nabla\Phi(s)|_\varepsilon).
\end{aligned}
$$

Using this notation, the parametrization (25) and the fact that $\partial\Phi(s)/\partial\nu = \Phi_x(s)$, we get that the integral along e_{pq_1} in term III_2 is equal to

$$\frac{h}{2}\sum_{i=1,2}\int_{-1}^{1}\Phi_x(s)\frac{m_{1i}(s)+n_{1i}(s)}{p_{1i}(s)}\,\mathrm{d}t. \tag{35}$$

For the edge e_{pq_3} we similarly obtain (denoting the variable on this edge by z)

$$a_{pq_3}^{n-1}-\frac{1}{|\nabla\Phi(z)|_\varepsilon}=\frac{1}{2}\Big(\frac{1}{|\nabla\Phi_{T_{31}}|_\varepsilon}-\frac{1}{|\nabla\Phi(z)|_\varepsilon}\Big)+\frac{1}{2}\Big(\frac{1}{|\nabla\Phi_{T_{32}}|_\varepsilon}-\frac{1}{|\nabla\Phi(z)|_\varepsilon}\Big),$$

$$\begin{aligned}\frac{1}{|\nabla\Phi(z)|_\varepsilon}-\frac{1}{|\nabla\Phi_{T_{31}}|_\varepsilon}=&\frac{((\Phi_p-\Phi_{q_3})/h-\Phi_x(z))((\Phi_p-\Phi_{q_3})/h+\Phi_x(z))}{|\nabla\Phi_{T_{31}}|_\varepsilon|\nabla\Phi(z)|_\varepsilon(|\nabla\Phi_{T_{31}}|_\varepsilon+|\nabla\Phi(z)|_\varepsilon)}\\&+\frac{(2(\Phi_{r_2}-\Phi_{m_3})/h-\Phi_y(z))(2(\Phi_{r_2}-\Phi_{m_3})/h+\Phi_y(z))}{|\nabla\Phi_{T_{31}}|_\varepsilon|\nabla\Phi(z)|_\varepsilon(|\nabla\Phi_{T_{31}}|_\varepsilon+|\nabla\Phi(z)|_\varepsilon)}\end{aligned}$$

and using again

$$\begin{aligned}\frac{\Phi_p-\Phi_{q_3}}{h}-\Phi_x(z)&=2\Phi_{xy}(z)t\frac{h}{2}+O(h^2),\\ \frac{2(\Phi_{r_2}-\Phi_{m_3})}{h}-\Phi_y(z)&=\Phi_{yy}(z)\frac{h}{2}(1-2t)+O(h^2),\end{aligned}$$

we can define

$$\begin{aligned}n_{3i}(z)&=\Big(2\Phi_{xy}(z)t\frac{h}{2}+O(h^2)\Big)\Big(\frac{\Phi_p-\Phi_{q_3}}{h}\Big)+\Phi_x(z),\\ m_{3i}(z)&=\Big(\Phi_{yy}(z)\frac{h}{2}(1-2t)+O(h^2)\Big)\Big(\frac{2(\Phi_{r_2}-\Phi_{m_3})}{h}+\Phi_y(z)\Big),\\ p_{3i}(z)&=|\nabla\Phi_{T_{3i}}|_\varepsilon|\nabla\Phi(z)|_\varepsilon(|\nabla\Phi_{T_{3i}}|_\varepsilon+|\nabla\Phi(z)|_\varepsilon).\end{aligned}$$

Now we get (notice that $\partial\Phi(z)/\partial\nu = -\Phi_x(z)$) that the integral along e_{pq_3} in term III_2 is equal to

$$-\frac{h}{2}\sum_{i=1,2}\int_{-1}^{1}\Phi_x(z)\frac{n_{3i}(z)+m_{3i}(z)}{p_{3i}(z)}\,\mathrm{d}t. \tag{36}$$

We can put together terms in (35) and (36) to obtain

$$\begin{aligned}
&\frac{h}{2}\sum_{i=1,2}\int_{-1}^{1}\Phi_x(s)\frac{m_{1i}(s)+n_{1i}(s)}{p_{1i}(s)}-\Phi_x(z)\frac{m_{3i}(z)+n_{3i}(z)}{p_{3i}(z)}\,\mathrm{d}t\\
&\qquad=\frac{h}{2}\sum_{i=1,2}\int_{-1}^{1}((\Phi_x(s)-\Phi_x(z))\frac{m_{1i}(s)+n_{1i}(s)}{p_{1i}(s)}\\
&\qquad\quad+\frac{h}{2}\sum_{i=1,2}\int_{-1}^{1}\Phi_x(z)\frac{m_{1i}(s)+n_{1i}(s)-(m_{3i}(z)+n_{3i}(z))}{p_{3i}(z)}\,\mathrm{d}t\\
&\qquad\quad+\frac{h}{2}\sum_{i=1,2}\int_{-1}^{1}\Phi_x(z)((m_{1i}(s)+n_{1i}(s))\Big(\frac{1}{p_{1i}(s)}-\frac{1}{p_{3i}(z)}\Big)\,\mathrm{d}t\\
&\qquad=IV_1+IV_2+IV_3.
\end{aligned}$$

In term IV_1 we can see that

$$\Big|\frac{m_{1i}(s)+n_{1i}(s)}{p_{1i}(s)}\Big|\leqslant\frac{C(\|\Phi\|_3)h}{|\nabla\Phi_{T_{1i}}|_\varepsilon|\nabla\Phi(s)|_\varepsilon}\leqslant\frac{C(\|\Phi\|_3)h}{\varepsilon|\nabla\Phi_{T_{1i}}|_\varepsilon}. \tag{37}$$

Since ε is fixed in our model and numerical scheme we get

$$|IV_1|\leqslant C(\|\Phi\|_3)h^3\Big(\frac{1}{|\nabla\Phi_{T_{11}}|_\varepsilon}+\frac{1}{|\nabla\Phi_{T_{12}}|_\varepsilon}\Big)$$

where C depends on ε. This dependence will not be explicitly stated in further estimates.

Term IV_2 can be estimated similarly. First we have

$$\begin{aligned}
&|m_{1i}(s)-m_{3i}(z)|\\
&\quad\leqslant\Big|\Big(\Phi_{yy}(s)\frac{h}{2}(1-2t)+O(h^2)\Big)\Big(\frac{2(\Phi_{r_1}-\Phi_{m_1})}{h}+\Phi_y(s)\Big)\\
&\qquad-\Big(\Phi_{yy}(z)\frac{h}{2}(1-2t)+O(h^2)\Big)\Big(\frac{2(\Phi_{r_2}-\Phi_{m_3})}{h}+\Phi_y(z)\Big)\Big|\\
&\quad\leqslant\Big|(\Phi_{yy}(z)-\Phi_{yy}(s))\frac{h}{2}(1-2t)+O(h^2)\Big|\,\Big|\frac{2(\Phi_{r_2}-\Phi_{m_3})}{h}+\Phi_y(z)\Big|\\
&\qquad+\Big|\Phi_{yy}(s)\frac{h}{2}(1-2t)+O(h^2)\Big|\\
&\qquad\times\Big|\Big(\frac{2(\Phi_{r_2}-\Phi_{m_3})}{h}+\Phi_y(z)\Big)-\Big(\frac{2(\Phi_{r_1}-\Phi_{m_1})}{h}+\Phi_y(s)\Big)\Big|
\end{aligned}$$

and analogously we can proceed with the term $|n_{1i} - n_{3i}|$. Then we get

$$
\begin{aligned}
|IV_2| &\leqslant C(\|\Phi\|_3)h^3 \sum_{i=1,2} \int_{-1}^{1} |\Phi_x(z)| \Big(\frac{|\nabla\Phi_{T_{3i}}|_\varepsilon + |\nabla\Phi(z)|_\varepsilon}{p_{3i}(z)} \Big) \\
&\quad + C(\|\Phi\|_2)h^3 \sum_{i=1,2} \int_{-1}^{1} \frac{|\Phi_x(z)|}{p_{3i}(z)} \\
&\leqslant C\|\Phi\|_3)h^3 \Big(\frac{1}{|\nabla\Phi_{T_{31}}|_\varepsilon} + \frac{1}{|\nabla\Phi_{T_{32}}|_\varepsilon} \Big) \\
&\quad + \frac{C(\|\Phi\|_3)h^3}{\varepsilon} \Big(\frac{1}{|\nabla\Phi_{T_{31}}|_\varepsilon} + \frac{1}{|\nabla\Phi_{T_{32}}|_\varepsilon} \Big) \\
&\leqslant C(\|\Phi\|_3)h^3 \Big(\frac{1}{|\nabla\Phi_{T_{31}}|_\varepsilon} + \frac{1}{|\nabla\Phi_{T_{32}}|_\varepsilon} \Big).
\end{aligned}
$$

For term IV_3 we get due to (37)

$$
\begin{aligned}
|IV_3| &\leqslant \frac{h}{2} \sum_{i=1,2} \int_{-1}^{1} |\Phi_x(z)| \frac{|(m_{1i}(s) + n_{1i}(s)||p_{3i}(z) - p_{1i}(s)|}{p_{1i}(s)p_{3i}(z)} \,\mathrm{d}t \\
&\leqslant C(\|\Phi\|_3)h^2 \sum_{i=1,2} \int_{-1}^{1} |\Phi_x(z)| \frac{|p_{3i}(z) - p_{1i}(s)|}{p_{3i}(z)|\nabla\Phi(s)|_\varepsilon |\nabla\Phi_{T_{1i}}|_\varepsilon} \,\mathrm{d}t.
\end{aligned}
$$

Now we first estimate

$$
\begin{aligned}
&|p_{3i}(z) - p_{1i}(s)| \\
&\quad = \big| |\nabla\Phi_{T_{3i}}|_\varepsilon^2 |\nabla\Phi(z)|_\varepsilon + |\nabla\Phi_{T_{3i}}|_\varepsilon |\nabla\Phi(z)|_\varepsilon^2 - (|\nabla\Phi_{T_{1i}}|_\varepsilon^2 |\nabla\Phi(s)|_\varepsilon \\
&\qquad\qquad + |\nabla\Phi_{T_{1i}}|_\varepsilon |\nabla\Phi(s)|_\varepsilon^2) \big| \\
&\quad \leqslant \big| |\nabla\Phi_{T_{3i}}|_\varepsilon^2 - |\nabla\Phi_{T_{1i}}|_\varepsilon^2 \big| |\nabla\Phi(s)|_\varepsilon + |\nabla\Phi_{T_{1i}}|_\varepsilon \big| |\nabla\Phi(s)|_\varepsilon^2 - |\nabla\Phi(z)|_\varepsilon^2 \big| \\
&\qquad + |\nabla\Phi_{T_{3i}}|_\varepsilon^2 \big| |\nabla\Phi(z)|_\varepsilon - |\nabla\Phi(s)|_\varepsilon \big| + |\nabla\Phi(z)|_\varepsilon^2 \big| |\nabla\Phi_{T_{3i}}|_\varepsilon - |\nabla\Phi_{T_{1i}}|_\varepsilon \big| \\
&\quad \leqslant C(\|\Phi\|_3)h \big| |\nabla\Phi(s)|_\varepsilon + |\nabla\Phi_{T_{1i}}|_\varepsilon \big| + C(\|\Phi\|_3)h(|\nabla\Phi_{T_{3i}}|_\varepsilon^2 + |\nabla\Phi(z)|_\varepsilon^2).
\end{aligned}
$$

Using this estimate we obtain

$$
\begin{aligned}
|IV_3| &\leqslant C(\|\Phi\|_3)h^4 \sum_{i=1,2} \int_{-1}^{1} \frac{|\Phi_x(z)| \big| |\nabla\Phi(s)|_\varepsilon + |\nabla\Phi_{T_{1i}}|_\varepsilon \big|}{p_{3i}(z)|\nabla\Phi(s)|_\varepsilon |\nabla\Phi_{T_{1i}}|_\varepsilon} \,\mathrm{d}t \\
&\quad + C(\|\Phi\|_3)h^3 \sum_{i=1,2} \int_{-1}^{1} \frac{|\Phi_x(z)|(|\nabla\Phi_{T_{3i}}|_\varepsilon^2 + |\nabla\Phi(z)|_\varepsilon^2)}{p_{3i}(z)|\nabla\Phi(s)|_\varepsilon |\nabla\Phi_{T_{1i}}|_\varepsilon} \,\mathrm{d}t
\end{aligned}
$$

$$
\begin{aligned}
&\leqslant C(\|\Phi\|_3)h^4 \sum_{i=1,2} \int_{-1}^{1} \frac{|\Phi_x(z)|}{p_{3i}(z)} \Big(\frac{1}{|\nabla\Phi_{T_{1i}}|_\varepsilon} + \frac{1}{|\nabla\Phi(s)|_\varepsilon} \Big) \\
&\quad + C(\|\Phi\|_3)h^3 \sum_{i=1,2} \int_{-1}^{1} \frac{|\Phi_x(z)-\Phi_x(s)|(|\nabla\Phi_{T_{3i}}|_\varepsilon + |\nabla\Phi(z)|_\varepsilon)^2}{p_{3i}(z)|\nabla\Phi(s)|_\varepsilon |\nabla\Phi_{T_{1i}}|_\varepsilon} \,\mathrm{d}t \\
&\quad + C(\|\Phi\|_3)h^3 \sum_{i=1,2} \int_{-1}^{1} \frac{|\Phi_x(s)|(|\nabla\Phi_{T_{3i}}|_\varepsilon + |\nabla\Phi(z)|_\varepsilon)^2}{p_{3i}(z)|\nabla\Phi(s)|_\varepsilon |\nabla\Phi_{T_{1i}}|_\varepsilon} \,\mathrm{d}t \\
&\leqslant \frac{C(\|\Phi\|_3)h^4}{\varepsilon} \sum_{i=1,2} \int_{-1}^{1} \frac{|\Phi_x(z)|}{p_{3i}(z)} + \frac{C(\|\Phi\|_3)h^4}{\varepsilon} \\
&\quad \times \sum_{i=1,2} \int_{-1}^{1} \frac{|\nabla\Phi_{T_{3i}}|_\varepsilon + |\nabla\Phi(z)|_\varepsilon}{|\nabla\Phi_{T_{3i}}|_\varepsilon |\nabla\Phi(z)|_\varepsilon |\nabla\Phi_{T_{1i}}|_\varepsilon} \,\mathrm{d}t \\
&\quad + C(\|\Phi\|_3)h^3 \sum_{i=1,2} \int_{-1}^{1} \frac{(|\nabla\Phi_{T_{3i}}|_\varepsilon + |\nabla\Phi(z)|_\varepsilon)}{|\nabla\Phi_{T_{3i}}|_\varepsilon |\nabla\Phi(z)|_\varepsilon |\nabla\Phi_{T_{1i}}|_\varepsilon} \,\mathrm{d}t \\
&\leqslant \frac{C(\|\Phi\|_3)h^4}{\varepsilon^2} \Big(\frac{1}{|\nabla\Phi_{T_{31}}|_\varepsilon} + \frac{1}{|\nabla\Phi_{T_{32}}|_\varepsilon} \Big) + \frac{C(\|\Phi\|_3)h^4}{\varepsilon^2} \Big(\frac{1}{|\nabla\Phi_{T_{11}}|_\varepsilon} + \frac{1}{|\nabla\Phi_{T_{12}}|_\varepsilon} \Big) \\
&\quad + \frac{C(\|\Phi\|_3)h^3}{\varepsilon} \Big(\frac{1}{|\nabla\Phi_{T_{11}}|_\varepsilon} + \frac{1}{|\nabla\Phi_{T_{12}}|_\varepsilon} \Big) \\
&\leqslant C(\|\Phi\|_3)h^4 \Big(\frac{1}{|\nabla\Phi_{T_{11}}|_\varepsilon} + \frac{1}{|\nabla\Phi_{T_{12}}|_\varepsilon} \Big) + C(\|\Phi\|_3)h^3 \Big(\frac{1}{|\nabla\Phi_{T_{11}}|_\varepsilon} + \frac{1}{|\nabla\Phi_{T_{12}}|_\varepsilon} \Big).
\end{aligned}
$$

If we use all these estimates for all edges in III_2 and use the relation (31) between b_p^{n-1} and a_{pq}^{n-1} we finally obtain

$$
|III_2| \leqslant C(\|\Phi\|_3)h + C(\|\Phi\|_3)h^2.
$$

In term III_1 we can use Green's theorem to obtain

$$
\begin{aligned}
III_1 = &-\frac{1}{b_p^{n-1} m(p)} \int_p \nabla \Big(\frac{\nabla\Phi(t_n,w)}{|\nabla\Phi(t_{n-1},w)|_\varepsilon} \Big) \,\mathrm{d}w \\
= &-\frac{1}{m(p)} \int_p \Big(\frac{1}{b_p^{n-1}} - |\nabla\Phi(t_{n-1},w)|_\varepsilon \Big) \nabla \cdot \Big(\frac{\nabla\Phi(t_n,w)}{|\nabla\Phi(t_{n-1},w)|_\varepsilon} \Big) \,\mathrm{d}w \\
&-\frac{1}{m(p)} \int_p |\nabla\Phi(t_{n-1},w)|_\varepsilon \nabla \cdot \Big(\frac{\nabla\Phi(t_n,w)}{|\nabla\Phi(t_{n-1},w)|_\varepsilon} \Big) \,\mathrm{d}w \\
= &-\frac{1}{m(p)} \int_p \Big(\frac{1}{b_p^{n-1}} - |\nabla\Phi(t_{n-1},w)|_\varepsilon \Big) \nabla \cdot \Big(\frac{\nabla\Phi(t_n,w)}{|\nabla\Phi(t_{n-1},w)|_\varepsilon} \Big) \,\mathrm{d}w \\
&- |\nabla\Phi(t_{n-1},\xi)|_\varepsilon \nabla \cdot \Big(\frac{\nabla\Phi(t_n,\xi)}{|\nabla\Phi(t_{n-1},\xi)|_\varepsilon} \Big) = V_1 + V_2
\end{aligned}
$$

where ξ is some point in the co-volume p from the mean value theorem. First we estimate the difference (again we omit for a moment the variable t_{n-1})

$$\left|\frac{1}{b_p^{n-1}} - |\nabla\Phi(w)|_\varepsilon\right| = \left|\frac{1/|\nabla\Phi(w)|_\varepsilon - b_p^{n-1}}{b_p^{n-1}\cdot 1/|\nabla\Phi(w)|_\varepsilon}\right|. \tag{38}$$

We can use (10) and (11) in the numerator of (38) and get

$$\begin{aligned}&\frac{1}{|\nabla\Phi(w)|_\varepsilon} - b_p^{n-1}\\ &\quad = \frac{1}{N_p}\sum_{q\in N(p)}\frac{1}{2}\Bigg(\Big(\frac{1}{|\nabla\Phi(w)|_\varepsilon} - \frac{1}{|\nabla\Phi_{T^1_{pq}}^{n-1}|_\varepsilon}\Big) + \Big(\frac{1}{|\nabla\Phi(w)|_\varepsilon} - \frac{1}{|\nabla\Phi_{T^2_{pq}}^{n-1}|_\varepsilon}\Big)\Bigg).\end{aligned}$$

From all terms in the sum we present the estimation of only one (concerning the triangle $T_{11} = T^1_{pq_1}$). The other terms can be treated in an analogous way. We use (12) and (34) to obtain

$$\begin{aligned}\left|\frac{1}{|\nabla\Phi_{T_{11}}|_\varepsilon} - \frac{1}{|\nabla\Phi(w)|_\varepsilon}\right| &= \left|\frac{|\nabla\Phi_{T^1_{pq_1}}|^2 - |\nabla\Phi(w)|^2}{|\nabla\Phi_{T_{11}}|_\varepsilon|\nabla\Phi(w)|_\varepsilon(|\nabla\Phi_{T_{11}}|_\varepsilon + |\nabla\Phi(w)|_\varepsilon)}\right|\\ &= \left|\frac{((\Phi_{q_1}-\Phi_p)/h)^2 - (\Phi_x(w))^2 + \big(2(\Phi_{r_1}-\Phi_{m_1})/h\big)^2 - (\Phi_y(w))^2}{|\nabla\Phi_{T_{11}}|_\varepsilon|\nabla\Phi(w)|_\varepsilon(|\nabla\Phi_{T_{11}}|_\varepsilon + |\nabla\Phi(w)|_\varepsilon)}\right|\\ &= \left|\frac{(\Phi_x(\xi)-\Phi_x(w))(\Phi_x(\xi)+\Phi_x(w)) + (\Phi_y(\zeta)-\Phi_y(w))(\Phi_y(\zeta)+\Phi_y(w))}{|\nabla\Phi_{T_{11}}|_\varepsilon|\nabla\Phi(w)|_\varepsilon(|\nabla\Phi_{T_{11}}|_\varepsilon + |\nabla\Phi(w)|_\varepsilon)}\right|.\end{aligned}$$

Now using the properties of Φ and the inequality $a+b \leqslant \sqrt{2}\sqrt{a^2+b^2+\varepsilon^2}$ holding for all $a \geqslant 0$, $b \geqslant 0$, we conclude

$$\left|\frac{1}{|\nabla\Phi_{T_{11}}|_\varepsilon} - \frac{1}{|\nabla\Phi(w)|_\varepsilon}\right| \leqslant \frac{C(\|\Phi\|_3)h}{|\nabla\Phi_{T_{11}}|_\varepsilon|\nabla\Phi(w)|_\varepsilon}.$$

Employing this type of estimates in (38) we have

$$\left|\frac{1}{b_p^{n-1}} - |\nabla\Phi(y)|_\varepsilon\right| \leqslant C(\|\Phi\|_3)h. \tag{39}$$

Now, the term V_1 can be rearranged to

$$\begin{aligned}V_1 = &-\frac{1}{m(p)}\int_p\Big(\frac{1}{b_p^{n-1}} - |\nabla\Phi(t_{n-1},w|_\varepsilon\Big)\frac{\Delta\Phi(t_n,w)}{|\nabla\Phi(t_{n-1},w)|_\varepsilon}\,\mathrm{d}w\\ &-\frac{1}{m(p)}\int_p\Big(\frac{1}{b_p^{n-1}} - |\nabla\Phi(t_{n-1},w|_\varepsilon\Big)\nabla\Phi(t_n,w)\cdot\nabla\Big(\frac{1}{|\nabla\Phi(t_{n-1},w)|_\varepsilon}\Big)\,\mathrm{d}w\\ = &\ V_{12}+V_{13}.\end{aligned}$$

The estimation of the term V_{12} is straightforward; due to the properties of Φ and the inequality (39) we get

$$|V_{12}| \leqslant C(\|\Phi\|_2)\frac{h}{\varepsilon} \leqslant C(\|\Phi\|_2)h.$$

For the term V_{13} we use

$$\nabla\Big(\frac{1}{|\nabla\Phi(t_{n-1},w)|_\varepsilon}\Big) = -\frac{1}{|\nabla\Phi(t_{n-1},w)|_\varepsilon^3}\boldsymbol{\Psi}(t_{n-1},w)$$

where for the two dimensional problem if $Z=(t_{n-1},w)$ then

$$\boldsymbol{\Psi}(Z) = \begin{pmatrix} \Phi_x(Z)\Phi_{xx}(Z)+\Phi_y(Z)\Phi_{xy}(Z) \\ \Phi_x(Z)\Phi_{xy}(Z)+\Phi_y(Z)\Phi_{yy}(Z) \end{pmatrix}$$

with the property

$$|\boldsymbol{\Psi}(Z)| \leqslant C(\|\Phi\|_2)|\nabla\Phi(Z)|. \tag{40}$$

Now for V_{13}, again taking into account the estimate (39) and the properties of Φ, we have

$$\begin{aligned}
|V_{13}| &\leqslant C(\|\Phi\|_2)h\frac{1}{m(p)}\int_p |\nabla\Phi(t_n,w)|\frac{1}{|\nabla\Phi(t_{n-1},w)|_\varepsilon^2}\,\mathrm{d}w \\
&\leqslant C(\|\Phi\|_2)h\frac{1}{m(p)}\int_p \big|\nabla\Phi(t_n,w)\pm|\nabla\Phi(t_{n-1},w)|\big|\frac{1}{|\nabla\Phi(t_{n-1},w)|_\varepsilon^2}\,\mathrm{d}w \\
&\leqslant C(\|\Phi\|_2)h\Big(\frac{\tau}{\varepsilon^2}+\frac{1}{\varepsilon}\Big) \leqslant C(\|\Phi\|_2)h + C(\|\Phi\|_2,\|\Phi\|_1)h\tau.
\end{aligned}$$

Finally, we couple together the term V_2 and the last term on the left-hand side of the inequality (24) and define

$$VI = -|\nabla\Phi(t_{n-1},\xi)|_\varepsilon\nabla\cdot\Big(\frac{\nabla\Phi(t_n,\xi)}{|\nabla\Phi(t_{n-1},\xi)|_\varepsilon}\Big) + |\nabla\Phi(X)|_\varepsilon\nabla\cdot\Big(\frac{\nabla\Phi(X)}{|\nabla\Phi(X)|_\varepsilon}\Big)$$

where $X=(t,x)$, the points x and ξ belong to the co-volume p and $t\in\langle t_{n-1},t_n\rangle$. Since

$$|\nabla\Phi(X)|_\varepsilon\nabla\cdot\Big(\frac{\nabla\Phi(X)}{|\nabla\Phi(X)|_\varepsilon}\Big) = \Delta\Phi(X) - \frac{\nabla\Phi(X)\cdot\boldsymbol{\Psi}(X)}{|\nabla\Phi(X)|_\varepsilon^2}$$

where the vector Ψ is defined as above, we obtain

$$|VI| \leqslant \Big|-\Delta\Phi(t_n,\xi) + \frac{\nabla\Phi(t_n,\xi)\cdot\boldsymbol{\Psi}(t_{n-1},\xi)}{|\nabla\Phi(t_{n-1},\xi)|_\varepsilon^2} + \Delta\Phi(X) - \frac{\nabla\Phi(X)\cdot\boldsymbol{\Psi}(X)}{|\nabla\Phi(X)|_\varepsilon^2}\Big|.$$

Because $|t - t_n| \leqslant \tau$ and $|x - \xi| \leqslant \sqrt{2}h$, we immediately have

$$|\Delta\Phi(X) - \Delta\Phi(t_n, \xi)| \leqslant C(\|\Phi\|_3)(\tau + h).$$

We rearrange the remaining terms to

$$\frac{\nabla\Phi(t_n,\xi)\cdot\boldsymbol{\Psi}(t_{n-1},\xi)}{|\nabla\Phi(t_{n-1},\xi)|_\varepsilon^2} \pm \frac{\nabla\Phi(X)\cdot\boldsymbol{\Psi}(t_{n-1},\xi)}{|\nabla\Phi(t_{n-1},\xi)|_\varepsilon^2} \pm \frac{\nabla\Phi(X)\cdot\boldsymbol{\Psi}(X)}{|\nabla\Phi(t_{n-1},\xi)|_\varepsilon^2} - \frac{\nabla\Phi(X)\cdot\boldsymbol{\Psi}(X)}{|\nabla\Phi(X))|_\varepsilon^2}.$$

Using the properties of Φ, $\boldsymbol{\Psi}$ and (40) we have

$$\begin{aligned}\Big|\frac{\nabla\Phi(t_n,\xi)\cdot\boldsymbol{\Psi}(t_{n-1},\xi)}{|\nabla\Phi(t_{n-1},\xi)|_\varepsilon^2} - \frac{\nabla\Phi(X)\cdot\boldsymbol{\Psi}(t_{n-1},\xi)}{|\nabla\Phi(t_{n-1},\xi)|_\varepsilon^2}\Big| &\leqslant \frac{C(\|\Phi\|_3)(h+\tau)|\nabla\Phi(t_{n-1},\xi)|}{|\nabla\Phi(t_{n-1},\xi)|_\varepsilon^2}\\ &\leqslant C(\|\Phi\|_3)(h+\tau).\end{aligned}$$

Now denoting $W = (t_{n-1}, \xi)$ we can use

$$\begin{aligned}&|\boldsymbol{\Psi}(W) - \boldsymbol{\Psi}(X)|\\ &\quad= \left|\begin{matrix}\Phi_x(W)\Phi_{xx}(W) + \Phi_y(W)\Phi_{xy}(W) - \Phi_x(X)\Phi_{xx}(X) - \Phi_y(X)\Phi_{xy}(X)\\ \Phi_x(W)\Phi_{xy}(W) + \Phi_y(W)\Phi_{yy}(W) - \Phi_x(X)\Phi_{xy}(X) - \Phi_y(X)\Phi_{yy}(X)\end{matrix}\right|\\ &\quad\leqslant C(|\Phi_x(W)\Phi_{xx}(W) + \Phi_y(W)\Phi_{xy}(W) - \Phi_x(X)\Phi_{xx}(X) - \Phi_y(X)\Phi_{xy}(X)|\\ &\qquad + |\Phi_x(W)\Phi_{xy}(W) + \Phi_y(W)\Phi_{yy}(W) - \Phi_x(X)\Phi_{xy}(X) - \Phi_y(X)\Phi_{yy}(X)|)\\ &\quad\leqslant C(\|\Phi\|_3)(h+\tau).\end{aligned}$$

Then we have

$$\begin{aligned}\Big|\frac{\nabla\Phi(X)\cdot\boldsymbol{\Psi}(t_{n-1},\xi)}{|\nabla\Phi(t_{n-1},\xi)|_\varepsilon^2} - \frac{\nabla\Phi(X)\cdot\boldsymbol{\Psi}(X)}{|\nabla\Phi(t_{n-1},\xi)|_\varepsilon^2}\Big|&\\ \leqslant \frac{C(\|\Phi\|_3)(h+\tau)|\nabla\Phi(X)|}{|\nabla\Phi(t_{n-1},\xi)|_\varepsilon^2}&\\ \leqslant C(\|\Phi\|_3)(h+\tau)\frac{|\nabla\Phi(X) \pm |\nabla\Phi(t_{n-1},\xi)|}{|\nabla\Phi(t_{n-1},\xi)|_\varepsilon^2}&\\ \leqslant C(\|\Phi\|_3)\Big(\frac{(h+\tau)^2}{\varepsilon^2} + \frac{h+\tau}{\varepsilon}\Big).&\end{aligned}$$

Finally, using (40) we successively get

$$
\begin{aligned}
&\Big|\frac{\nabla\Phi(X)\cdot\mathbf{\Psi}(X)}{|\nabla\Phi(t_{n-1},\xi)|_\varepsilon^2}-\frac{\nabla\Phi(X)\cdot\mathbf{\Psi}(X)}{|\nabla\Phi(X))|_\varepsilon^2}\Big|\\
&\qquad\qquad\leqslant|\nabla\Phi(X)\cdot\mathbf{\Psi}(X)|\Big|\frac{|\nabla\Phi(X)|^2-|\nabla\Phi(t_{n-1},\xi)|^2}{|\nabla\Phi(X)|_\varepsilon^2|\nabla\Phi(t_{n-1},\xi)|_\varepsilon^2}\Big|\\
&\qquad\qquad\leqslant C(\|\Phi\|_2)(h+\tau)|\nabla\Phi(X)|^2\\
&\qquad\qquad\quad\times\Big(\frac{1}{|\nabla\Phi(X)|_\varepsilon|\nabla\Phi(t_{n-1},\xi)|_\varepsilon^2}+\frac{1}{|\nabla\Phi(X)|_\varepsilon^2|\nabla\Phi(t_{n-1},\xi)|_\varepsilon}\Big)\\
&\qquad\qquad\leqslant C(\|\Phi\|_2)(h+\tau)\Big(\frac{|\nabla\Phi(X)\pm\nabla\Phi(t_{n-1},\xi)|}{|\nabla\Phi(t_{n-1},\xi)|_\varepsilon^2}+\frac{1}{|\nabla\Phi(t_{n-1},\xi)|_\varepsilon}\Big)\\
&\qquad\qquad\leqslant C(\|\Phi\|_3)\Big(\frac{(h+\tau)^2}{\varepsilon^2}+\frac{h+\tau}{\varepsilon}\Big)\leqslant C(\|\Phi\|_3)((h+\tau)^2+(h+\tau)),
\end{aligned}
$$

which completes the proof. $\square$

References

[1] *L. Alvarez, F. Guichard, P.-L. Lions, J.-M. Morel*: Axioms and fundamental equations of image processing. Arch. Ration. Mech. Anal. *123* (1993), 200–257. zbl

[2] *S. Angenent, M. E. Gurtin*: Multiphase thermomechanics with an interfacial structure. 2. Evolution of an isothermal interface. Arch. Ration. Mech. Anal. *108* (1989), 323–391. zbl

[3] *G. Barles, P. E. Souganidis*: Convergence of approximation schemes for fully nonlinear second order equations. Asymptotic Anal. *4* (1991), 271–283. zbl

[4] *M. Beneš, K. Mikula*: Simulations of anisotropic motion by mean curvature—comparison of phase field and sharp interface approaches. Acta Math. Univ. Comen. *67* (1998), 17–42.

[5] *S. L. Chan, E. O. Purisima*: A new tetrahedral tesselation scheme for isosurface generation. Computers and Graphics *22* (1998), 83–90.

[6] *V. Caselles, R. Kimmel, G. Sapiro*: Geodesic active contours. International Journal of Computer Vision *22* (1997), 61–79. zbl

[7] *Y.-G. Chen, Y. Giga, S. Goto*: Uniqueness and existence of viscosity solutions of generalized mean curvature flow equation. J. Differ. Geom. *33* (1991), 749–786. zbl

[8] *S. Corsaro, K. Mikula, A. Sarti, F. Sgallari*: Semi-implicit co-volume method in 3D image segmentation. SIAM J. Sci. Comput. *28* (2006), 2248–2265. zbl

[9] *M. G. Crandall, H. Ishii, P.-L. Lions*: User's guide to viscosity solutions of second order partial differential equations. Bull. Am. Math. Soc. (NS) *27* (1992), 1–67. zbl

[10] *K. Deckelnick, G. Dziuk*: Error estimates for a semi-implicit fully discrete finite element scheme for the mean curvature flow of graphs. Interfaces Free Bound. *2* (2000), 341–359. zbl

[11] *K. Deckelnick, G. Dziuk*: Numerical approximations of mean curvature flow of graphs and level sets. In: Mathematical Aspects of Evolving Interfaces (L. Ambrosio, K. Deckelnick, G. Dziuk, M. Mimura, V. A. Solonnikov, H. M. Soner, eds.). Springer, Berlin-Heidelberg-New York, 2003, pp. 53–87. zbl

[12] *G. Dziuk*: An algorithm for evolutionary surfaces. Numer. Math. *58* (1991), 603–611. zbl

[13] *G. Dziuk*: Convergence of a semi-discrete scheme for the curve shortening flow. Math. Models Methods Appl. Sci. *4* (1994), 589–606. zbl

[14] *L. C. Evans, J. Spruck*: Motion of level sets by mean curvature I. J. Differ. Geom. *33* (1991), 635–681. zbl
[15] *A. Handlovičová, K. Mikula, A. Sarti*: Numerical solution of parabolic equations related to level set formulation of mean curvature flow. Comput. Vis. Sci. *1* (1998), 179–182. zbl
[16] *A. Handlovičová, K. Mikula, F. Sgallari*: Semi-implicit complementary volume scheme for solving level set like equations in image processing and curve evolution. Numer. Math. *93* (2003), 675–695. zbl
[17] *A. Handlovičová, K. Mikula, F. Sgallari*: Variational numerical methods for solving nonlinear diffusion equations arising in image processing. J. Visual Communication and Image Representation *13* (2002), 217–237.
[18] *J. Kačur, K. Mikula*: Solution of nonlinear diffusion appearing in image smoothing and edge detection. Appl. Numer. Math. *17* (1995), 47–59. zbl
[19] *S. Kichenassamy, A. Kumar, P. Olver, A. Tannenbaum, A. Yezzi*: Conformal curvature flows: from phase transitions to active vision. Arch. Ration. Mech. Anal. *134* (1996), 275–301. zbl
[20] *R. Le Veque*: Finite Volume Methods for Hyperbolic Problems. Cambridge Texts in Applied Mathematics. Cambridge University Press, Cambridge, 2002.
[21] *K. Mikula, J. Kačur*: Evolution of convex plane curves describing anisotropic motions of phase interfaces. SIAM J. Sci. Comput. *17* (1996), 1302–1327. zbl
[22] *K. Mikula, N. Ramarosy*: Semi-implicit finite volume scheme for solving nonlinear diffusion equations in image processing. Numer. Math. *89* (2001), 561–590. zbl
[23] *K. Mikula, A. Sarti, F. Sgallari*: Co-volume method for Riemannian mean curvature flow in subjective surfaces multiscale segmentation. Comput. Vis. Sci. *9* (2006), 23–31.
[24] *K. Mikula, A. Sarti, F. Sgallari*: Semi-implicit co-volume level set method in medical image segmentation. In: Handbook of Biomedical Image Analysis: Segmentation and Registration Models (J. Suri et al., eds.). Springer, New York, 2005, pp. 583–626.
[25] *K. Mikula, D. Ševčovič*: Evolution of plane curves driven by a nonlinear function of curvature and anisotropy. SIAM J. Appl. Math. *61* (2001), 1473–1501. zbl
[26] *K. Mikula, D. Ševčovič*: Computational and qualitative aspects of evolution of curves driven by curvature and external force. Computing and Visualization in Science *6* (2004), 211–225.
[27] *R. H. Nochetto, M. Paolini, C. Verdi*: Sharp error analysis for curvature dependent evolving fronts. Math. Models Methods Appl. Sci. *3* (1993), 711–723. zbl
[28] *A. M. Oberman*: A convergent monotone difference scheme for motion of level sets by mean curvature. Numer. Math. *99* (2004), 365–379. zbl
[29] *S. Osher, R. Fedkiw*: Level Set Methods and Dynamic Implicit Surfaces. Springer, New York, 2003.
[30] *S. Osher, J. Sethian*: Fronts propagating with curvature-dependent speed: Algorithms based on Hamilton-Jacobi formulations. J. Comput. Phys. *79* (1988), 12–49. zbl
[31] *A. Sarti, R. Malladi, J.A. Sethian*: Subjective surfaces: A method for completing missing boundaries. Proc. Natl. Acad. Sci. USA *12* (2000), 6258–6263. zbl
[32] *J. A. Sethian*: Level Set Methods and Fast Marching Methods. Evolving Interfaces in Computational Geometry, Fluid Mechanics, Computer Vision, and Material Science. Cambridge University Press, New York, 1999. zbl
[33] *N. J. Walkington*: Algorithms for computing motion by mean curvature. SIAM J. Numer. Anal. *33* (1996), 2215–2238. zbl

Authors' address: *A. Handlovičová, K. Mikula*, Department of Mathematics, Slovak University of Technology, Radlinského 11, 813 68 Bratislava, Slovakia, e-mail: `angela@math.sk`, `mikula@math.sk`.